A Novel Four-Dimensional Modulation Format Based on Subset Selection

GUIJUN HU AND ZHAOXI LI

Department of Communication Engineering, Jilin University, Changchun 130012, China

Corresponding author: Zhaoxi Li (lzx23@jlu.edu.cn)

ABSTRACT Coherent optical transmission systems have a four-dimensional (4-D) signal space (two quadratures in two polarizations), which can be used to create 4-D modulation formats that have better sensitivity than traditional two-dimensional modulation signal. In this paper, we propose an interesting four-dimensional modulation format based on subset selection for coherent optical fiber communications. We compare the proposed modulation format to the polarization multiplexed quadrature amplitude modulation(PM-QAM) and the set-partitioning M polarization-multiplexed QAM (M-SP-QAM). Simulation results show that for the same spectral efficiency, the proposed modulation format can get SNR gains of up to1dB compared with PM-MQAMs at 7% forward exchange control (FEC) threshold at a BER of 1e-3 in back-to-back system. After 800 km transmission distance, the signal-to-noise ratio (SNR) gain is 1.05dB. It is also shown that the mapping process of the proposed modulation format has lower latency and occupies less memory units compared with the commonly used look-up-tables mapping method.

INDEX TERMS Digital modulation, high-dimensional modulation, optical communication.

I. INTRODUCTION

In recent years, coherent detection has been widely used in optical communication, since it is feasible to implement at high data rates. Also, it provides access to the four dimension signal space (two quadratures in two polarizations) for data transmission. More recently, efforts have been made to improve the performance of coherent optical systems by considering joint modulation of all four dimensions of the carrier, which is often called a four-dimensional modulation format (4D). Compare to the 2D modulation formats such as PM-APSK [1] and PM-MQAM [2], the joint modulation method can optimize the constellation in 4D spanned to achieve larger minimum Euclidean distance between symbols [3]–[5]. That is, a four-dimensional modulation format can improve the sensitivity at little expense of spectral efficiency and providing an effective solution to the trade-off between spectral efficiency and sensitivity [6]–[9].

Since 2009, Bülow, Agrell, and Karlsson proposed many power efficiency modulation formats [10]–[12]. Agrell proposed the polarization-switched quad-phase shift key (PS-QPSK) which has the most power-efficient modulation

---

The associate editor coordinating the review of this manuscript and approving it for publication was Lei Guo.

format in fiber optic communication systems [13], [14]. Further gains can be obtained by generalized pulse-position modulation or by coding [15], [16]. Furthermore, Bülow [17] has demonstrated polarization-QAM (POL-QAM) modulation, which is an extension of PM-QPSK to six polarization states with one additional bit per two PM-QPSK symbols. Coelho and Hanik [18] introduced two additional modulation formats to the fiber optic communication research community by applying the Ungerboeck set-partitioning scheme to PM-16QAM. These formats were called set-partitioning 32 PM-16-QAM (32-SP-QAM) [19] and set-partitioning 128 PM-16-QAM (128-SP-QAM)[20]. But, this M-SP-QAM always results in the odd number of encoded bits per symbol. All of the above formats mapping is look-up-table (LUT) mapping. The latency and the storage cost of LUT are huge with the increasing of the modulation dimensional and spectral efficiency (SE)[21]. So, for the higher modulation dimensional formats, their SE is limited. Thus, a fast mapping with lower latency and space complexity is needed when the high dimensional modulation formats are designed.

Comprehensive considering the power efficiency and the mapping method, we propose a four-dimensional modulation format based on subset selection, named subset selection p bit four dimension (SS-pb4D), which carries p ($p = 4n$, $n<Z^+$)

bit information per symbol. Z^+ represents positive integer. The basic design idea of the modulation format is to divide the four-dimensional constellation point set into several subsets, and increase the minimum Euclidean distance between the constellation points by selecting the constellation points in each subset, to improve the power efficiency of the modulation format. Fast mapping is achieved by establishing the function of bit label and constellation point coordinate. The mapping process is formulaic, the computational time complexity is independent of the size of the constellation point set, and the storage cost is small. In this paper, the bit error performance and de-mapping complexity of the proposed four-dimensional modulation format are analyzed and verified. The simulation results show that compared with the existing PM-MQAM, the proposed 4D modulation format can achieve better signal-to-noise ratio gain without a reduction of SE. Compared with the LUT mapping method, the latency and storage cost of the fast detection and de-mapping process for the proposed format are significantly reduced.

The paper is organized as follows. In Section 2, we explain the principle of SS-pb4D modulation formats, including the design of the SS-pb4D constellation set and fast mapping and de-mapping process. And Section 3 provides the simulation results. We evaluate the error performance of SS-8b4D, SS-12b4D, PM-16QAM, and PM-64QAM, and compare the basic calculated amount of the proposed de-mapping and LUTs de-mapping method. Finally, conclusions are drawn in Section 4.

II. PRINCIPLE OF SS-pb4D MODULATION FORMAT

The binary source sequence L_p is broken up into p-bit labeling $B_1, B_2, \cdots B_k \cdots, B_L$ where p denotes the number of bits per labeling. Then each bit labeling B_k is mapped to one of the four-dimensional constellation points by $S_k = \Gamma(B_k)$, where $k \in [1, L]$, Γ is a formalized mapping rule, $M = 2^p$ is the number of constellation points, and each S_k is selected from the constellation set $C = \{c_1, c_2, \cdots, c_e, \cdots, c_M\}$ of SS-pb4D format. In general, the union bound on the Symbol Error Rate (SER) can be expressed as eq(1)[22].

$$\text{SER} \leq \frac{1}{M} \sum_{k=1}^{M} \sum_{\substack{lj=1 \\ j \neq k}}^{M} \frac{1}{2} \text{erfc}(\frac{d_{kj}}{2\sqrt{N_0}}) \quad (1)$$

In which, a function of the distance $d_{kj} = \|c_k - c_j\|$, and $d_{\min} = \min_{j \neq k} d_{kj}$ is the minimum Euclidean distance of the constellation. In order to compare the performance of constellations with different numbers of levels at a fixed bit rate R, the dominant term of eq(1) can be rewritten as $erfc(\sqrt{E_b \gamma / (R N_0)})$, where $\gamma = d_{\min}^2 / 4 E_b$, $E_b = E_s / \log_2 M$, E_s is average energy per bit. M is the number of constellation points. N_0 is the energy of noise. The parameter γ is called the Asymptotic Power Efficiency (APE), the power needed for a certain required SER is proportional to $1/\gamma$ [23]. So, in order to find the best constellation with the maximum APE,

the location of the constellation points should be designed. Moreover, the constellation points should meet the requirements of fast mapping. So, in this section, we describe the design of SS-pb4D including the location of constellation points and the mapping method.

A. THE DESIGN OF THE SS-pb4D CONSTELLATION SET

The design of the SS-pb4D is based on a 4D set-partitioning (SP) scheme, for SP scheme, the constellation points are the subset of certain states out of the possible states from a dual-polarization M-QAM constellation. So, though the $d_{\min}$ of SP-M-QAM is increased, the SE is reduced since the possible combination states are removed. Fig 1 (a) is the constellation points in one polarization direction (x or y), all the possible states of the combination of the red round points in the two polarization direction are made up to be the SP-M-QAM constellation points. Thus, the $d_{\min}$ of SP-M-QAM is $2\sqrt{2}$. We call the combination of red round points in the two polarization direction sets A. For the SP-M-QAM modulation format, the constellation can be expanded in 2D MQAM constellation when much more points are needed. It can be seen from the process, some possible combination states points whose $d_{\min}$ are $2\sqrt{2}$ neglected. For example, the $d_{\min}$ of the 4D constellation points which are combined by the triangle points and the round points are also $2\sqrt{2}$ (we call it sets B). The combination of star points and the round points are as well (we call it the sets C). The constellation of SS-pb4D modulation formats is just the union of the sets A, B and C. Next, how to map the bit label into these constellation points needs to be designed.

Firstly, we define the coordinates of the constellation of SS-pb4D as $[p_0, p_1]$. Here, p_0 is the coordinates of constellation points in x polarization, and p_1 is the y direction $p_1 = [c_2, c_3]$. Fig 1 gives different 2D constellation for one polarization direction of SS-pb4D. In order to meet the $d_{\min} = 2\sqrt{2}$, the value of c_i should be selected from the set:

$$\varphi_n^2 = \{(c_i) \in 2h(h \in Z) : c^{2q} + c^{2q+1} \equiv 0 (\text{mod}2)(q = 0, 1)\}$$

The steps of the design for SS-p b4D constellation set are given as follows:

1) Set the targeted number of constellation points: $M = 2^p = 2^{4n}(n \geq 2 \& n \in Z^+)$;

2) Calculate the needed number of the SS-pb4D 2D constellation points: $N_m = 3 \cdot 2^{2n-1}$;

3) Select N_m points as 2D constellation set of SS-pb4D that is defined as φ_n^2. In Fig 1 (c), 2D constellations sets of SS-pb4D are divided into three regions, named N_1(like the red round points), N_{2-1}(the red star points), and N_{2-2}(the red triangle points), respectively.

4) Divide 2D constellations set of SS-pb4Dφ_n^2 into two subsets, named B_I and B_{II}:

$$B_I = \{(c^i) \in \varphi_n^2 : c^{2q} + c^{2q+1} \equiv 0 (\text{mod}4)\}, q \in \{0, 1\} \quad (2)$$

$$B_{II} = \{(c^i) \in \varphi_n^2 : c^{2q} + c^{2q+1} \equiv 2 (\text{mod}4)\}, q \in \{0, 1\} \quad (3)$$

As shown in the Fig 1 (a), (b) and (c), the red and blue shaped markers represent B_I and B_{II}, respectively.

(a)

(b)

(c)
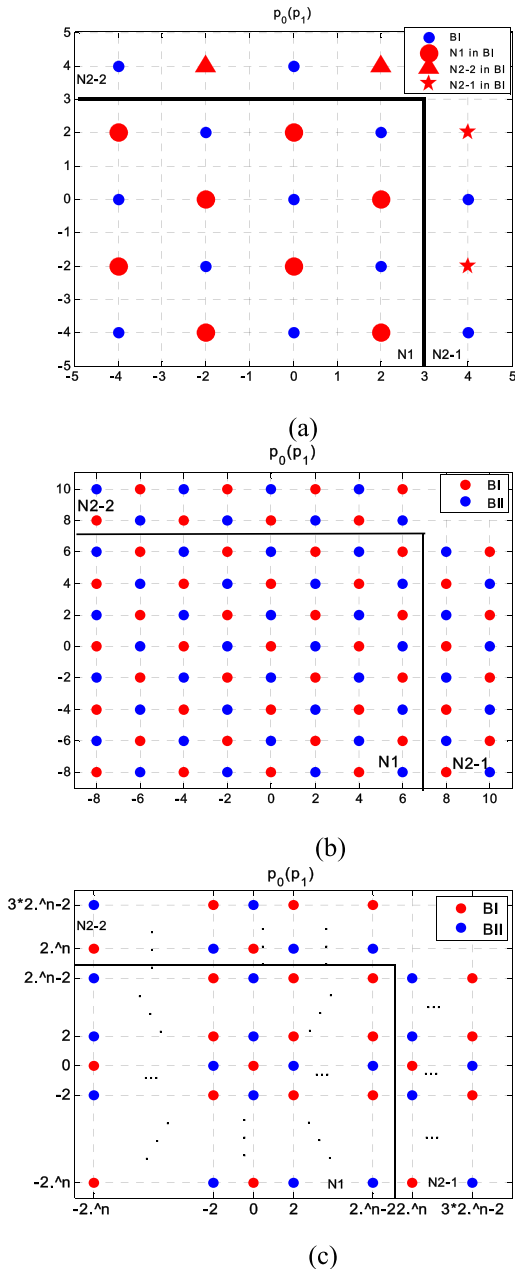
FIGURE 1. (a) 2D constellation design scheme of SS-8b4D: φ_2^2. (b) 2D constellation design schemeof SS-12b4D: φ_3^2. (c) 2D constellation design scheme of SS-pb4D: φ_n^2.

5) Calculate the five SS-pb4D constellation subsets:

$$C_I = [p_0, p_1]^T, \quad \begin{matrix} p_0 \in B_{I,N_1}, p_1 \in B_{I,N_1} \text{ or} \\ p_0 \in B_{II,N_1}, p_1 \in B_{II,N_1} \end{matrix} \quad (4)$$

$$C_{II} = [p_0, p_1]^T, \quad \begin{matrix} p_0 \in B_{I,N_1}, p_1 \in B_{I,N_{2-1}} \text{ or} \\ p_0 \in B_{II,N_1}, p_1 \in B_{II,N_{2-1}} \end{matrix} \quad (5)$$

$$C_{III} = [p_0, p_1]^T, \quad \begin{matrix} p_0 \in B_{I,N_1}, p_1 \in B_{I,N_{2-2}} \text{ or} \\ p_0 \in B_{II,N_1}, p_1 \in B_{II,N_{2-2}} \end{matrix} \quad (6)$$

$$C_{IV} = [p_0, p_1]^T, \quad \begin{matrix} p_0 \in B_{I,N_{2-1}}, p_1 \in B_{I,N_1} \text{ or} \\ p_0 \in B_{II,N_{2-1}}, p_1 \in B_{II,N_1} \end{matrix} \quad (7)$$

$$C_V = [p_0, p_1]^T, \quad \begin{matrix} p_0 \in B_{I,N_{2-2}}, p_1 \in B_{I,N_1} \text{ or} \\ p_0 \in B_{II,N_{2-2}}, p_1 \in B_{II,N_1} \end{matrix} \quad (8)$$

TABLE 1. The SE and APE of SS-pb4D which n is equal to 2 and 3, and corresponding to PM-MQAM and M-SP-QAM.

	M	SE (b/s/Hz/pol)	APE (dB)
SS-8b4D	256	4	-2.58
128ary-SP-QAM	128	3.5	-1.55
PM-16QAM	16	4	-3.97
SS-12b4D	4096	6	-6.99
2048ary-SP-QAM	2048	5.5	-5.98
PM-64QAM	64	6	-8.45

where B_{I,N_1} is a subset of B_I in the N_1 region, $B_{I,N_{2-1}}$ and $B_{I,N_{2-1}}$ are the subset of B_I in the N_{2-1} and N_{2-2} region respectively, in the same way, B_{II,N_1}, $B_{II,N_{2-1}}$ and $B_{II,N_{2-2}}$ are subset of B_{II} in N_1, N_{2-1} and N_{2-2} regions respectively.

6) Finally, we get the constellation set of SS-pb4D: $C = C_I \cup C_{II} \cup C_{III} \cup C_{IV} \cup C_V$.

Therefore, in the Fig 1 (a), the subset coordinate of C_I to C_V are expressed as follows. Select one point among the 8 red round points in x polarization direction, and select another one point among 8 in y polarization direction, the two 2D points can combine into a 4D point. Thus, there will be $C_8^1 \cdot C_8^1 = 64$ possible combination; they are the points in C_I. Then, select one point among the 8 red round points in x polarization direction and select one point among the 2 red star points, there will be $C_8^1 \cdot C_2^1 = 16$ possible combination; they are the points in C_{II}. In the same way, C_{III} to C_V has $C_8^1 \cdot C_2^1 = 16$ points respectively. Thus, the red points can combine $C_8^1 \cdot C_8^1 + C_8^1 \cdot C_2^1 + C_8^1 \cdot C_2^1 + C_8^1 \cdot C_2^1 + C_8^1 \cdot C_2^1 = 128$ points. The blue points can also combine into 128 points. So the 256 points of SS-8b4D can be achieved.

In TABLE 1, we compute the APE and SE of PM-16QAM and SS-8p4D. It can be seen from that compared to PM-16QAM, SS-8b4D has about 1.39dB APE gain without reducing of SE. SS-12b4D has about 1.46dB APE gain compared to the PM-64QAM.

Additionally, much more points can be selected than M-SP-QAM in unit volume by using the proposed constellation points design method. So, compared to M-SP-QAM, the proposed SS-pb4D is closer to the Shannon limit [24]. Fig 2. gives the SE and $1/\gamma$ (γ is the APE) curves for different modulation formats. It can be seen from Fig 2. that the proposed SS-pb4D is closer to the Shannon limit than PM-MQAM and M-SP-QAM, and it can encode even numbers of bits per symbol.

B. FAST MAPPING AND DE-MAPPING METHOD OF SS-PB4D MODULATION FORMAT

For 4D modulation formats, except for designing the locations of the constellation points to improve the APE, another problem is how to map the bits to symbols and re-map the bits from the received symbols. Most of the high-dimensional modulation format achieves this by using the LUT, which
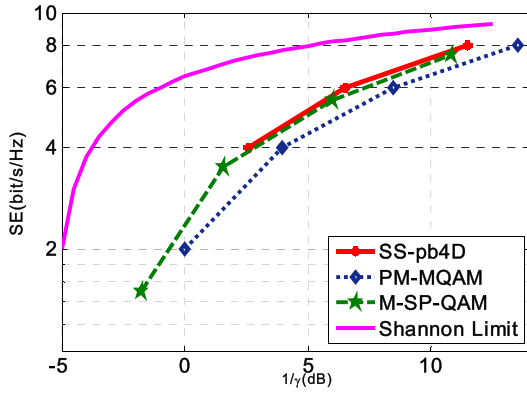
FIGURE 2. A Comparison between the SE&$1/\gamma$ for different modulation formats under the Shannon Limit.

TABLE 2. The bit-to-symbol mapping of SS-pb4D.

b_0	b_1	b_2	b_3	b_4	...	b_{4n-2}	b_{4n-1}
0	C_{I}						
1	0	0	C_{II}				
1	0	1	C_{III}				
1	1	0	C_{IV}				
1	1	1	C_{V}				

will introduce much more latency and occupies memory units when the size of the constellation is large. So, how to realize the fast mapping and de-mapping through building the formula between the bits and symbols is important for designing a high-dimensional modulation formats.

1) BIT-TO-SYMBOL MAPPING

The symbol mapping for these bits is explained in TABLE 2. Denoting the b_0, b_1, b_2 as the bits for subset selection, we distinguish between five cases, depending on whether b_0, b_1, b_2(or b_0) belongs to the five cases. After selecting the subset, the bit labeling for each coordinate value of a constellation point in the selected subset can be encoded according to Fig 3.

The details of mapping are as follows: the bit-to-symbol mapping is defined as $\Gamma : B_k \rightarrow S_k$, and corresponding symbol-to-bit de-mapping is $\Gamma^{-1} : S_k \rightarrow B_k$. The 4D code vector is $S_k = [s_0, s_1, s_2, s_3]^T$, the bit label is $b_e(b_e \in B_k = [b_0, b_1, \ldots, b_e, \ldots, b_{4n-1}])^T$. Firstly, every $4n$ bits are mapped to a 4D point. We divide the 2^{4n} constellation points into five subsets, which are C_{I} to C_{V}, the first bit b_0 is used for the subset selection, when $b_0 = 0$, C_{I} is selected, then b_1-b_{4n-1} and the check bit P_{N_1} can get from mathematical equation in the flowchart in Fig 3. Next, according to value of P_{N_1}, the vector S_k can be calculated through the formulas in Fig 3. Significantly, though this method, the two 4D constellation points with the minimum Euclidean distance can get the minimum bit difference. The flowchart of the mapping method is given in Fig 3.
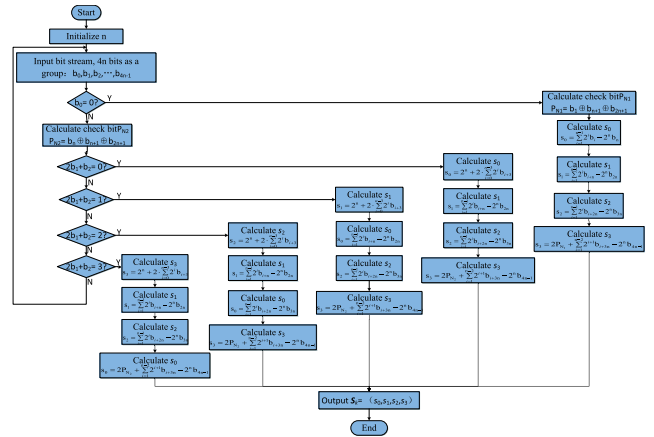

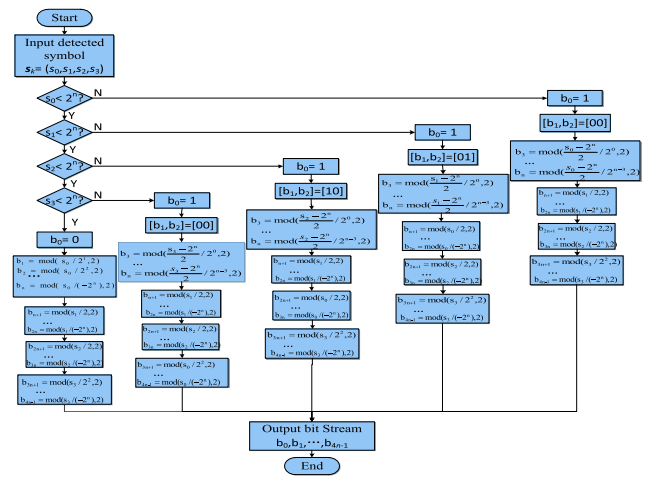**FIGURE 3.** The flowchart of the mapping method for SS-pb4D modulation format.

FIGURE 4. The flowchart of de-mapping method for SS-pb4D modulation format.

2) DETECTION AND DE-MAPPING

At the receiver, the received signal is described by $R_k = S_k + N_k$, where N_k is the zero-mean Gaussian noise with variance σ^2. S_k can get from the Sphere Decoding algorithm [25]. In Fig 4 we give the process that how to de-map the S_k into the bit labels. Meanwhile, the de-mapping Γ^{-1} can get from Fig 4.

During the de-mapping process, a $4n$-bit block is recovered from one detected symbol. The three bits, b_0, b_1 and b_2, are decoded according to the Subset Selection. Therefore, b_0, b_1 and b_2 are identified in terms of the boundary value of the coordinate of the detected symbol, i.e. 2^n. When the coordinate of code vectors $s_0 \geq 2^n$, the detected symbol lies in C_{II} subset, so, b_0, b_1, and b_2 are equal to 1, 0 and 0 respectively. And b_3-b_{4n-1} can be got. In this way, when the coordinate of code vectors $s_1 \geq 2^n$, $s_2 \geq 2^n$ or $s_3 \geq 2^n$, the detected symbol lies in C_{III}, C_{IV} or C_{V} subset respectively. In this way, the bit label can get from the flowchart instead of checking the table of bit-to-symbol. Thus, it has lower latency and occupies less memory units compared with the commonly used LUT mapping method.
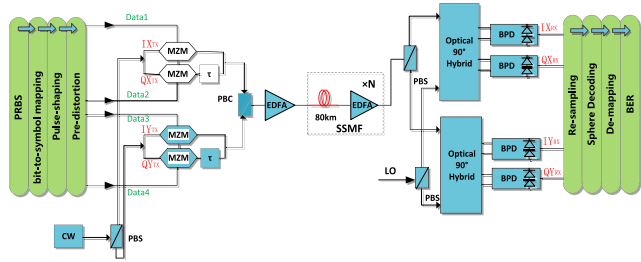
FIGURE 5. The block diagram of the four-dimensional transmission system.

III. SIMULATION RESULTS AND PERFORMANCE COMPARISON ANALYSIS

A. TRANSMISSION PERFORMANCE ANALYSIS

In this paper, the simulation performed in VPI. The block diagram of the four-dimensional transmission system is shown in Fig 5. At the transmitter, we use a continuous wave laser (CW) with a line width of 100 kHz as the laser source. The generated sequences of the normalized four-dimensional symbols are split into four parts and modulated by a dual-polarization I/Q modulator with the real and imaginary parts of each of the two orthogonal polarizations. And the sequences are pre-calculated with a raised cosine pulse shaping with a roll-off factor of 0.88 and repeatedly transmitted. The modulated data streams are transmitted 800km over a standard single-mode fiber (SSMF). The SSMF parameters are as follows: Attenuation coefficient is 0.2dB/km, chromatic dispersion is 16ps/nm/km, polarization mode dispersion is 0.2ps/nm/km, and the Erbium-doped fiber amplifier (EDFA) noise figure is set to 5.0 dB. At the receiver, polarization diversity is obtained by splitting the signal with a polarization beam-splitter (PBS) and mixing the light in the x- and the y-polarization with the output from a local oscillator (LO) laser in two optical 90° hybrids having integrated balanced detectors. After photo-detection, the received signals are sampled by ADCs and sent to MATLAB for offline digital signal process (DSP). In this paper, we follow the same approach as [25] for impairment compensation. Finally, BER is a measure for performance evaluation.

The performance of SS-8b4D and SS-12b4D are simulated under the back-to-back (B2B) system and 800km transmission system respectively, PM-MQAM is as a reference for the same SE. And the simulation sets the same symbol rate of 14Gbaud; The SNR gains of these modulation formats with 7% overhead (OH) FEC threshold at BER of 10^{-3} are compared.

The B2B system simulation results for the formats are shown in Fig 6. Substantially, SS-8b4D and SS-12b4D outperforms PM-16QAM and PM-64QAM by about 1 dB at the 7% OH FEC limits. In Fig 6(a), at the FEC limit 10^{-3}, the measured optical signal to noise ratio (OSNR) for SS-8b4D and PM-16QAM is 16.9dB and 17.8dB respectively. Therefore, SS-8b4D requires about 0.9dB less OSNR than PM-16QAM. And the result also shows SS-12b4D outperforms PM-64QAM by about 1dB less OSNR required at the targeted BER of 10^{-3} in Fig 6 (b).
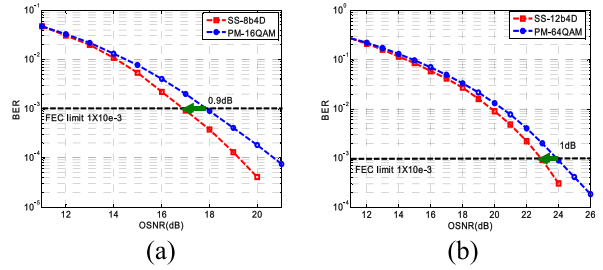

FIGURE 6. (a) BER vs OSNR in B2B for SS-8b4D and PM-16QAM. (b) BER vs OSNR in B2B for SS-12b4D and PM-16QAM.
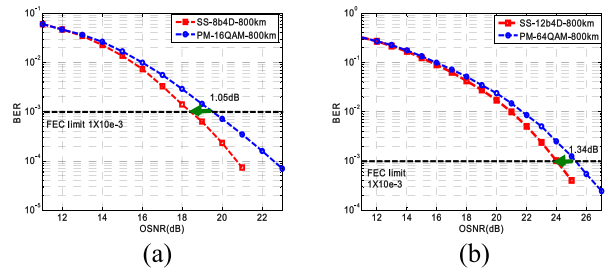

FIGURE 7. (a) BER as a function of OSNR of the transmission results after a 800 km transmission distance. (b) BER as a function of OSNR of the transmission results after a 800 km transmission distance.

Fig 7 (a) and (b) show the BER performance comparison results of SS-8b4D and PM-16QAQM, as well as that of SS-12b4D and PM-64QAM after 800 km transmission at the 7% OH FEC limits, respectively. Compared with the performance of B2B system, the two modulation formats in Fig 7 (a) have about 1.58dB and 1.66dB transmission OSNR penalty respectively. And the other two modulation formats in Fig 7 (b) have 1.02dB and 1.21dB transmission OSNR penalty respectively. Thus the proposed formats have better transmission performance compare to conventional PM-MQAMs with the same as spectral efficiency. Moreover, the simulation results also show SS-8b4D and SS-12b4D have 1.05dB and 1.34dB sensitivity gains than PM-16QAM and PM-64QAM respectively. Therefore, the sensitivity gain of SS-12b4D is larger than SS-8b4D with low spectral efficiency by 0.29dB at the 7% OH FEC limits. And we can see that the proposed formats have about 1dB improvement on the BER performance compared with the conventional PM-MQAM.

The transmission results for 10.5 Gbaud PM-MQAM, M-SP-QAM and SS-pb4D for single channel transmission are shown in Fig 8, the optimal launch power is -1dBm. It can be seen from Fig 8 that the proposed formats SS-pb4D give an increase in transmission distance for a receiver BER of 1e-3 compared to PM-MQAM for the same SE. It is also shown that, when the SE increases from 4bit/s/Hz/pol, to 6 bit/s/Hz/pol, SS-pb4D can get greater gain in transmission distance than PM-MQAM. The explanation for the behavior is that when it expands the constellation in the lattice structure in a certain volume, the d_{min} of PM-MQAM decreases faster than SS-pb4D at the same SE, because the
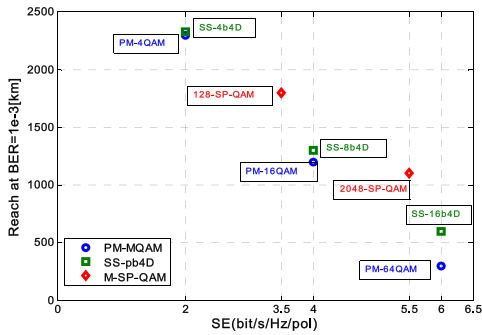
FIGURE 8. Transmission results for different modulation formats.

subset selection method can get much more points which satisfied the required $d_{\min}$. Likewise, in virtue of the subset selection method can get much more points with the same $d_{\min}$ than M-SP-QAM in unit volume. So, compared with M-SP-QAM and PM-MQAM, the SS-pb4D can get a trade-off between SE and transmission distance.

B. CALCULATED AMOUNT OF DE-MAPPING METHOD ANALYSIS

For 4D modulation formats, de-mapping and detections will bring much more amount of searching calculation, especially for the modulation formats of higher SE, the required memory unit increase exponentially when the LUT is commonly used in de-mapping. For the proposed SS-pb4D formats, the bits labels can decode from the detected symbols though Fig 4. The constellation needn't save in the memory units.

For the amount of calculation of detection and de-mapping, we compare the proposed de-mapping method with the LUTs de-mapping method in terms of the basic calculation amount, which means the total number of arithmetical operation [27]. We can define the basic calculated amount as Fc. And then in TABLE 3, the calculated amount of receiving comes from the de-mapping and symbol detection. The complexity of the Sphere Decoding decision presented in [28], and then the number of arithmetical operations is

$$O(N^2 \times (1 + \frac{N-1}{4Dd})^{4Dd}) \quad (9)$$

where, the same fixed search radius is used d as [24]. The complexity is obviously independent of the constellation size, i.e. the number of operations does not depend on the spectral efficiency of the signal constellation. Therefore, the calculated amount can be expressed as $O(N^6)$. And the basic calculated amount of the de-mapping method is the function of n according to flowchart in Fig 4. Thus the comprehensive calculated amount is $N^6 \times (2^{n-2} + 34n6)$.The calculated amount of LUTs de-mapping with the same decision method is $N^6 \times (24n + 4n)$ in TABLE 3.

Fig 9 shows the general trend of F_c with the increase of n for the proposed method and the LUTs respectively. In Fig 9, when n is equal to 3, namely the constellation points are $M = 2^p = 2^{4n} = 4096$, F_c of the LUTs demonstrates a trend of rapid increase, while F_c of the proposed method demonstrates slow growth. And compared to the proposed

TABLE 3. Comparison of the proposed de-mapping and the LUTs de-mapping method and detection in terms of the basic calculated amount (the comprehensive calculated amount D is that calculated amount of detection Det(N,n) and calculated amount of de-mapping De-(N,n) are multiplied, i.e., D= Det(N,n)×De-(N,n). The complexity of LUTs de-mapping with the same decision method is shown as a comparison).

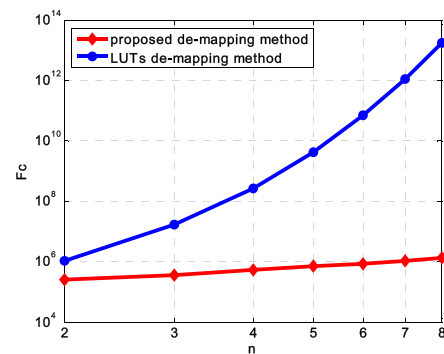|	Addition		Multiplication		totality
	Det(N,n)	De-(N,n)	Det(N,n)	De-(N,n)	D
proposed de-mapping	-	$2^{n-2}+7n+3$	N^6	$25n-9$	$N^6\times(2^{n-2}+34n-6)$
LUTs de-mapping	-	$2^{4n}+4n$	N^6	-	$N^6\times(2^{4n}+4n)$

FIGURE 9. F_c vs n for proposed de-mapping and LUTs de-mapping and symbol detection.

method with the LUTs, a reduction of four orders of magnitude is offered when n is equal to 5.The results also show that the basic calculated amount of the fast mapping method is not restricted by the number of constellation points, e.g. M. Therefore, this method makes it possible to realize the high-dimensional modulation formats which have higher spectral efficiency.

IV. CONCLUSION
In this paper, we propose an interesting four-dimensional modulation format based on subset selection SS-pb4D for coherent optical transmission system. This format can get higher power efficiency than PM-MQAM without reduction of SE, and it can realize fast mapping though establishing the formal between bit label and symbols. The simulation results show that the proposed formats have about 1dB improvement on the BER performance compared with the conventional PM-MQAMs at 7% OH FEC limits 10^{-3}. It is also shown that the basic calculated amount of the proposed format detection and de-mapping is much lower than that of LUTs, considering the requirements on capacity, power efficiency, fast (de-)mapping and flexibility, SS-pb4D is a possible candidate for the coherent optical interconnections.

REFERENCES
[1] G. Charlet, J. Renaudier, H. Mardoyan, P. Tran, O. B. Pardo, F. Verluise, A. Boutin, F. Blache, J.-Y. Dupuy, and S. Bigo, "Transmission of 16.4-bit/s capacity over 2550 km using PDM QPSK modulation format and coherent receiver," *J. Lightw. Technol.*, vol. 27, no. 3, pp. 153–157, Feb. 1, 2009.

[2] P. J. Winzer, A. H. Gnauck, C. R. Doerr, M. Magarini, and L. L. Buhl, "Spectrally efficient long-haul optical networking using 112-Gb/s polarization-multiplexed 16-QAM," *J. Lightw. Technol.*, vol. 28, no. 4, pp. 547–556, Feb. 15, 2010.

[3] S. Betti, F. Curti, G. De Marchis, and E. Iannone, "A novel multilevel coherent optical system: 4-Quadrature signaling," *J. Lightw. Technol.*, vol. 9, no. 4, pp. 514–523, Apr. 1991.

[4] K. Kojima, T. Yoshida, T. Koike-Akino, D. S. Millar, K. Parsons, and V. Arlunno, "5 and 7 bit/symbol 4D modulation formats based on 2A8PSK," in *Proc. 42nd Eur. Conf. Opt. Commun.*, Sep. 2016, pp. 1–3.

[5] J. Renaudier, O. Bertran-Pardo, A. Ghazisaeidi, P. Tran, H. Mardoyan, P. Brindel, A. Voicila, G. Charlet, and S. Bigo, "Experimental transmission of Nyquist pulse shaped 4-D coded modulation using dual polarization 16QAM set-partitioning schemes at 28 Gbaud," in *Proc. Opt. Fiber Commun. Conf. Expo. Nat. Fiber Optic Eng. Conf.*, Mar. 2013, pp. 1–3.

[6] X. Lu, A. Tatarczak, V. Lyubopytov, and I. T. Monroy, "Optimized eight-dimensional lattice modulation format for IM-DD 56 Gb/s optical interconnections using 850 nm VCSELs," *J. Lightw. Technol.*, vol. 35, no. 8, pp. 1407–1414, Apr. 15, 2017.

[7] G. Ungerboeck, "Channel coding with multilevel/phase signals," *IEEE Trans. Inf. Theory*, vol. 28, no. 1, pp. 55–67, Jan. 1982.

[8] G. D. Forney, "Multidimensional constellations. II. Voronoi constellations," *IEEE J. Sel. Areas Commun.*, vol. 7, no. 6, pp. 941–958, Aug. 1989.

[9] T. A. Eriksson, S. Alreesh, C. Schmidt-Langhorst, F. Frey, P. W. Berenguer, C. Schubert, J. K. Fischer, P. A. Andrekson, M. Karlsson, and E. Agrell, "Experimental investigation of a four-dimensional 256-ary lattice-based modulation format," in *Proc. Opt. Fiber Commun. Conf. Exhib.*, Mar. 2015, pp. 1–3.

[10] E. Agrell and M. Karlsson, "Power-efficient modulation formats in coherent transmission systems," *J. Lightw. Technol.*, vol. 27, no. 22, pp. 5115–5126, Nov. 15, 2009.

[11] D. Millar, D. Lavery, S. Makovejs, C. Behrens, B. C. Thomsen, P. Bayvel, and S. J. Savory, "Generation and long-haul transmission of polarization-switched QPSK at 42.9 Gb/s," *Opt. Express*, vol. 19, no. 10, pp. 9296–9302, 2011.

[12] D. S. Millar, T. Koike-Akino, S. Ö. Arik, K. Kojima, and K. Parsons, "Comparison of quaternary block-coding and sphere-cutting for high-dimensional modulation," in *Proc. Opt. Fiber Commun. Conf. Exhib.*, Mar. 2014, pp. 1–3.

[13] M. Karlsson and E. Agrell, "Which is the most power-efficient modulation format in optical links?" *Opt. Express*, vol. 17, no. 13, pp. 10814–10819, Jun. 2009.

[14] M. Nölle, J. K. Fischer, L. Molle, C. Schmidt-Langhorst, D. Peckham, and C. Schubert, "Comparison of 8 × 112 Gb/s PS-QPSK and PDM-QPSK signals over transoceanic distances," *Opt. Express*, vol. 19, no. 24, pp. 24370–24375, 2011.

[15] D. S. Millar, T. Koike-Akino, S. Ö. Arik, K. Kojima, K. Parsons, T. Yoshida, and T. Sugihara, "High-dimensional modulation for coherent optical communications systems," *Opt. Express*, vol. 22, no. 7, pp. 8798–8812, Apr. 2014.

[16] S. Alreesh, C. Schmidt-Langhorst, R. Emmerich, P. W. Berenguer, C. Schubert, and J. K. Fischer, "Four-dimensional trellis coded modulation for flexible optical communications," *J. Lightw. Technol.*, vol. 35, no. 2, pp. 152–158, Jan. 15, 2017.

[17] H. Bülow, "Polarization QAM modulation (POL-QAM) for coherent detection schemes," in *Proc. Conf. Opt. Fiber Commun.*, Mar. 2009, pp. 1–3.

[18] L. D. Coelho and N. Hanik, "Global optimization of fiber-optic communication systems using four-dimensional modulation formats," in *Proc. 37th Eur. Conf. Expo. Opt. Commun.*, Sep. 2011, pp. 1–3.

[19] T. A. Eriksson, M. Sjödin, P. A. Andrekson, and M. Karlsson, "Experimental demonstration of 128-SP-QAM in uncompensated long-haul transmission," in *Proc. Opt. Fiber Commun. Conf. Expo. Nat. Fiber Optic Eng. Conf.*, Mar. 2013, pp. 1–3.

[20] R. Rios-Muller, J. Renaudier, O. Bertran-Pardo, A. Ghazisaeidi, P. Tran, G. Charlet, and S. Bigo, "Experimental comparison between hybrid-QPSK/8QAM and 4D-32SP-16QAM formats at 31.2 GBaud using Nyquist pulse shaping," in *Proc. 39th Eur. Conf. Exhib. Opt. Commun.*, Sep. 2013, pp. 1–3.

[21] Y. Dong, J. Zhang, Z. Wang, K. Staenz, C. Coburn, W. Xu, X. Yang, and J. Wang, "Method to speed up LUT-based crop canopy parameter mapping," in *Proc. IEEE Geosci. Remote Sens. Symp.*, Jul. 2014, pp. 2078–2081.

[22] S. Benedetto and E. Biglieri, *Principles of Digital Transmission: With Wireless Applications*. Norwell, MA, USA: Kluwer, 1999.

[23] J. H. Conway and N. J. A. Sloane, *Sphere Packings, Lattices, and Groups*, 3rd ed. New York, NY, USA: Springer, 1998.

[24] S. Ishimura and K. Kikuchi, "Multi-dimensional permutation modulation aiming at both high spectral efficiency and high power efficiency," in *Proc. Opt. Fiber Commun. Conf.*, Mar. 2014, pp. 1–3.

[25] E. Viterbo and J. Boutros, "A universal lattice code decoder for fading channels," *IEEE Trans. Inf. Theory*, vol. 45, no. 5, pp. 1639–1642, Jul. 1999.

[26] H. Büelow, T. Rahman, F. Buchali, W. Idler, and W. Kuebart, "Transmission of 4-D modulation formats at 28-Gbaud," in *Proc. Opt. Fiber Commun. Conf. Expo. Nat. Fiber Optic Eng. Conf.*, Mar. 2013, pp. 1–3.

[27] L. Brunel and J. J. Boutros, "Lattice decoding for joint detection in direct-sequence CDMA systems," *IEEE Trans. Inf. Theory*, vol. 49, no. 4, pp. 1030–1037, Apr. 2003.

[28] U. Fincke and M. Pohst, "Improved methods for calculating vectors of short length in a lattice, including a complexity analysis," *Math. Comput.*, vol. 44, no. 170, pp. 463–471, Apr. 1985.

GUIJUN HU was born in Liaoning, China, in 1970. He received the B.S. and M.S. degrees in optical engineering from the University of Northeast Normal University, in 1996, and the Ph.D. degree in microelectronics and solid state electronics from Jilin University.

From 2000 to 2005, he was a Senior Lecturer with the Department of Communication Engineering, Jilin University, where he has been a Professor, since 2006. He is the author of more than 100 articles and more than ten inventions. His research interests include optical fiber communication, optoelectronics, and fiber sensor. He is a member of the Society of Photo-Optical Instrumentation Engineers (SPIE).

ZHAOXI LI received the B.Sc. degree in communication engineering and the M.Sc. degree in signal and information processing, in 2007 and 2009, respectively, and the Ph.D. degree from Jilin University. She was with industry as a Scientific Research Engineer, for seven years. She is currently a Senior Engineer with the Department of Communication Engineering, Jilin University. She became involved in multidisciplined research. Her main interests include optical fiber communication system and signal processing.

● ● ●